Acta Cryst. (1976). B32, 2163

Combined X-ray and Neutron Diffraction Studies of Normal and Deuterated Iminodiacetic Acid Hydrobromide

BY Å. OSKARSSON

Inorganic Chemistry 1, *Chemical Center, University of Lund, P.O.B.* 740, *S*-220 07 *Lund* 7, *Sweden*

(*Received* 29 *December* 1975; *accepted* 24 *January* 1976)

The structures of $C_4H_8NO_4Br$ and $C_4H_4D_4NO_4Br$ have been investigated at room temperature by X-ray ($\lambda = 1{\cdot}5418$ Å) and neutron diffraction ($\lambda = 1{\cdot}210$ Å). The compounds are isostructural, crystallizing in the space group *Pmmn* with $Z = 2$ and $a = 12{\cdot}8150$, $b = 5{\cdot}8707$, $c = 5{\cdot}0870$ Å and $a = 12{\cdot}8047$, $b = 5{\cdot}8670$, $c = 5{\cdot}0807$ Å, respectively. Positively charged iminodiacetic acid ions are connected by hydrogen bonds O–H···Br and N–H···Br forming layers that are stacked in the **c** direction. The forces between the layers are van der Waals. (X–N) difference syntheses have been calculated for the normal compound to illustrate the electron density within the organic ion and in the hydrogen bonds.

Introduction

In a systematic study of the geometry of the positively charged iminodiacetic acid ion, $[C_4H_8NO_4]^+$, the structures of the addition compounds of iminodiacetic acid with the hydrogen halides have been determined from X-ray intensities (Oskarsson, 1973, 1974*a*,*b*). They contain chains of positively charged iminodiacetic acid ions and halide ions, linked by hydrogen bonds into layers. The forces between the layers are van der Waals. These compounds decompose at very different rates when stored in contact with air at room temperature. The stability increases in the series F < Cl < Br < I. The F compound decomposes within 24h (Oskarsson, 1974*b*) and the Cl within two months (Oskarsson, 1974*c*). The decomposition is accompanied by release of the hydrogen halide according to: $H_3LX(s) \rightarrow H_2L(s) + HX(g)$, where $L = C_4H_5NO_4^{2-}$. However, in the chloride a more stable compound is obtained when the acid H atoms are replaced by D. Kinetic hydrogen isotope effects have been reviewed by Bell (1974). The theoretical models for this phenomenon have often been based on the assumption that potential energy curves or surfaces are unaffected by isotopic substitution. The structures of normal and deuterated iminodiacetic acid hydrochloride have been studied previously by X-ray methods (Oskarsson, 1973, 1974*c*). It was concluded that the two hydrogen bonds N–H···Cl and O–H···Cl are shortened on deuteration and as a consequence the potential energy curves for both N–H···Cl and O–H···Cl are affected by isotopic substitution in this compound.

The structure of iminodiacetic acid hydrobromide (IDAB) has been studied previously by X-ray diffraction (Oskarsson, 1973). The present work was undertaken to determine the H positions in IDAB and the D positions in deuterated iminodiacetic acid hydrobromide (DIDAB), in order to study the geometry of the bonds N–H···Br, O–H···Br and N–D···Br, O–D···Br. Another purpose of this investigation is to use the atomic coordinates obtained in the neutron studies for analyses of the X-ray intensity data sets to illustrate the electron density within the organic ion and in the hydrogen bonds. This technique has previously been applied to only one compound containing a third row element, namely Cr (Rees & Coppens, 1973).

Crystal data

IDAB, $C_4H_8NO_4Br$: F.W. 214·04. Orthorhombic, *Pmmn*; $a = 12{\cdot}8150$ (20),* $b = 5{\cdot}8707$ (7), $c = 5{\cdot}0870$ (7) Å, $V = 382{\cdot}70$ Å^3, $Z = 2$. DIDAB, $C_4H_4D_4NO_4Br$: F.W. 218·04. Orthorhombic, *Pmmn*; $a = 12{\cdot}8047$ (33), $b = 5{\cdot}8670$ (16), $c = 5{\cdot}0807$ (12) Å, $V = 381{\cdot}69$ Å^3, $Z = 2$.

Experimental

Large single crystals of IDAB were grown by slow evaporation at room tempreature of a solution of iminodiacetic acid in hydrobromic acid. The crystal data are taken from Oskarsson (1973). The volume of the crystal used in the data collection was 9·42 mm^3 and it had eight well formed faces. The intensities were collected at room temperature with a computer-controlled Hilger & Watts four-circle diffractometer at the R2 reactor, Studsvik, Sweden. For this instrument the flux of the monochromatic neutron beam at the specimen is about 10^6 n cm^{-2} s^{-1} and the wave length is 1·210 Å. Two sets of data were recorded with the ω–2θ step scan technique. The first consists of two octants of the reflexion sphere out to $\sin\theta/\lambda = 0{\cdot}53$ Å^{-1}, the second of one octant in the range $0{\cdot}53 < \sin\theta/\lambda < 0{\cdot}69$ Å^{-1}. Two standard reflexions per set were measured at regular intervals to provide a check on crystal and electronic stabilities. About 15 min were spent measuring each reflexion. The values of I and $\sigma_c(I)$ were corrected for Lorentz and absorption ef-

* Numbers in parentheses represent estimated standard deviations in the last significant digits.

fects. The standard deviations $\sigma_o(I)$ were based on counting statistics. Two of the boundary planes of the crystal used were large and parallel, (100) and ($\bar{1}$00), and an experimental linear absorption coefficient was determined (1·477 cm^{-1}). This value corresponds to an incoherent scattering cross section for H of 35 barns. The transmission factors evaluated by numerical integration varied from 0·68 to 0·85.

Crystals of DIDAB were grown by repeated recrystallization of IDAB from a solution of DBr in D_2O containing more than 99·5% D. Powder photographs were taken with a Guinier–Hägg focusing camera (Cu $K\alpha_1$ radiation, $\lambda = 1{\cdot}54051$ Å). The spectra were indexed with the lattice parameters of IDAB. The unit-cell dimensions were then improved by least-squares refinement.

A single crystal with a volume of 41·93 mm^3 was mounted in a thin-walled quartz bulb and used for the data collection with the same experimental conditions as for IDAB. Only data from one octant of the reflexion sphere out to $\sin\theta/\lambda = 0{\cdot}69$ $Å^{-1}$ were collected. The linear absorption coefficient was experimentally determined from the parallel boundary planes (100) and ($\bar{1}$00). The value obtained was 0·497 cm^{-1} corresponding to an incoherent scattering cross section of 24 barns for hydrogen. The transmission factors varied from 0·80 to 0·92.

A single crystal of DIDAB, 0·12 × 0·25 × 0·20 mm, was mounted in a thin-walled Lindeman glass capillary. X-ray intensities were collected on a computer-controlled four-circle diffractometer of type CAD-4. Experimental conditions and data reduction were as described previously (Oskarsson, 1973) with one exception: the scan interval, $\Delta\omega$, was extended 25% at both ends for background measurement with moving crystal and detector. All 430 reflexions in the range $5° < \theta < 70°$ were measured. The transmission factors varied from 0·24 to 0·46 [μ(Cu $K\alpha$) = 76·7 cm^{-1}].

Refinement

The parameters given by Oskarsson (1973) were used in the preliminary refinements to minimize the function $\sum w(|F_o| - |F_c|)^2$ with weights $w^{-1} = \sigma_c^2/4|F_o|^2 + a|F_o|^2$, with the constant a approximately 10^{-3} for all three data sets. The final refinements were based on F^2 and weights used were $w^{-1} = \sigma_c^2 + b|F_o|^4$. Reflexions with $I < 0$ were given zero weight. The X-ray data set was corrected for isotropic extinction, while the neutron data sets were also tested for anisotropic extinction (Zachariasen, 1967). In the anisotropic models the exinction depends on six parameters (Coppens & Hamilton, 1970). The extinction is governed by mosaic spread for type 1 and by particle size for type 2 crystals. Some characteristics of the refinements are given in Table 1. It was concluded that the extinction was dominated by domain size for IDAB with the parameters 3·12, 6·25 and 5·28 μm. There was no significant difference between type 1 and type 2 for DIDAB, and type 2 was chosen arbitrarily. The domain size was 3·79, 3·83 and 3·87 μm.

Table 1. *Some characteristics of the refinements*

		Model I*	Model II	Model III
IDAB	$R(F^2)$	0·093	0·075	0·062
(Neutron)	$R_w(F^2)$	0·104	0·088	0·077
	S†	1·7	1·4	1·2
	b‡	0·0009	0·0009	0·001
DIDAB	$R(F^2)$	0·086	0·075	0·076
(Neutron)	$R_w(F^2)$	0·105	0·096	0·097
	S	2·3	2·0	2·0
	b	0·0007	0·0008	0·0008
DIDAB	$R(F^2)$	0·064		
(X-ray)	$R_w(F^2)$	0·078		
	S	3·4		
	b	0·0003		

* Model I is isotropic extinction correction and models II and III are anisotropic extinction corrections of types 1 and 2, respectively (Zachariasen, 1967).

† $S = [\sum w(|F_o|^2 - |F_c|^2)^2/(m-n)]^{1/2}$, where m is the number of observations and n the number of parameters varied.

‡ b is a constant in the weighting function. See text.

In the last cycles of the refinements, the shifts in the parameters were less than 2% of the estimated standard deviations and the refinements were considered complete. The average values of $w(|F_o|^2 - |F_c|^2)^2$ were nearly constant in the different $|F_o|^2$ intervals. The coherent scattering amplitudes used were taken from Bacon (1972), and the scattering factors from

Table 2. *Positional parameters with estimated standard deviations*

	x	y	z
IDAB, neutron			
Br	¼	¾	0·55290 (53)
N	¼	¼	0·26151 (30)
O(1)	0·43093 (16)	¼	0·52049 (38)
O(2)	0·52783 (16)	¼	0·15540 (43)
C(1)	0·43936 (12)	¼	0·28539 (30)
C(2)	0·34651 (12)	¼	0·10299 (30)
H(1)	¼	0·10995 (70)	0·38204 (66)
H(2)	0·34776 (20)	0·10181 (76)	−0·02209 (68)
H(3)	0·58652 (28)	¼	0·27817 (82)
DIDAB, neutron			
Br	¼	¾	0·55316 (72)
N	¼	¼	0·26082 (35)
O(1)	0·43088 (21)	¼	0·51961 (45)
O(2)	0·52749 (19)	¼	0·15391 (53)
C(1)	0·43917 (14)	¼	0·28473 (37)
C(2)	0·34646 (15)	¼	0·10175 (36)
D(1)	¼	0·10912 (51)	0·38318 (48)
H(2)	0·34786 (33)	0·10189 (99)	−0·02146 (80)
D(3)	0·58628 (20)	¼	0·27831 (57)
DIDAB, X-ray			
Br	¼	¾	0·55319 (10)
N	¼	¼	0·26016 (61)
O(1)	0·43087 (24)	¼	0·52003 (47)
O(2)	0·52748 (21)	¼	0·15358 (49)
C(1)	0·43863 (25)	¼	0·28560 (56)
C(2)	0·34656 (28)	¼	0·10229 (60)
D(1)	¼	0·1332 (64)	0·3743 (78)
H(2)	0·3487 (28)	0·1199 (72)	0·0005 (47)
D(3)	0·5668 (34)	¼	0·2308 (91)

Hanson, Herman, Lea & Skillman (1964) (Br^-, C, N, O); Stewart, Davidson & Simpson (1965) (H); and *International Tables for X-ray Crystallography* (1974) (f' and f'' for Br). The positional and thermal parameters, and the r.m.s. components along the principal axes of the thermal motion ellipsoids, are given in Tables 2 and 3.* All computations were made on the Univac 1108 computer in Lund, Sweden, and the program system used has been described by Oskarsson (1973).

Half-normal probability plot analysis

Positional and thermal parameters have been compared by the method of half-normal probability plots (Abrahams & Keve, 1971). This method is convenient in detecting minor differences in two sets of parameters. Observed ranked values of $\delta p_i = ||p(1)_i| - |p(2)_i||/[\sigma^2 p(1)_i + \sigma^2 p(2)_i]^{1/2}$ are plotted *versus* the quantiles ξ_i, expected for a normal distribution of errors. The values of ξ_i are calculated according to Hamilton & Abrahams (1972). The quantities $p(1)_i$ and $p(2)_i$ are the corresponding parameters in sets 1 and 2, respectively, with the estimated standard deviations $\sigma p(1)_i$ and $\sigma p(2)_i$. Besides information about differences in the compared parameter sets, these plots might also give information about the reliability of the standard deviations assigned to the parameters. A linear plot with a slope of unity and zero intercept may be interpreted as a correct match between measured and assumed error distribution in two equivalent sets of parameters. Plots with other shapes indicate either errors in the estimation of $\sigma p_i = [\sigma^2 p(1) + \sigma^2 p(2)_i]^{1/2}$ or systematic differences between the two sets of parameters. The plots discussed below were obtained by the program *PPCPAR* (Albertsson, 1974).

Comparisons of the parameters from the neutron investigations of IDAB and DIDAB gave linear plots (Fig. 1). The slope of the line for the positional parameters indicates that the standard deviations are not underestimated by more than 20% in either IDAB or DIDAB. The intercept shows a small but perhaps significant difference between the two data sets. If this is the case, there is either a small systematic experimental error present in one of the two data sets or there is an isotope effect on the positional parameters. The plot for the thermal parameters shows significant differences between the two data sets, which is to be expected because of the different masses of H and D.

The results of the X-ray and the neutron data sets are given in Figs. 2 and 3 [the X-ray parameters for IDAB were taken from Oskarsson (1973)]. The plots for the positional parameters are linear with a slope of 1·04 for both IDAB and DIDAB, which indicates

* A list of structure factors has been deposited with the British Library Lending Division as Supplementary Publication No. SUP 31638 (7 pp.). Copies may be obtained through The Executive Secretary, International Union of Crystallography, 13 White Friars, Chester CH1 1NZ, England.

Table 3. *Thermal parameters* $\beta_{ij} \times 10^4$ *and r.m.s. components* R_i *along the principal axes of the ellipsoids of thermal vibration*

The expression used is $\exp[-(\beta_{11}h^2 + \ldots + 2\beta_{12}hk + \ldots)]$. The temperature factors of H and D were not refined in the X-ray study, but given an arbitrary value of 3·0 Å².

	β_{11}	β_{22}	β_{33}	β_{12}	β_{13}	β_{23}	R_1	R_2	R_3
IDAB, neutron									
Br	37 (1)	207 (7)	449 (11)	0	0	0	0·176 (3)	0·190 (3)	0·243 (3)
N	33 (1)	215 (5)	216 (6)	0	0	0	0·163 (3)	0·168 (3)	0·194 (2)
O(1)	45 (1)	452 (9)	232 (8)	0	−4 (2)	0	0·174 (3)	0·194 (3)	0·281 (3)
O(2)	37 (1)	401 (9)	311 (8)	0	15 (2)	0	0·168 (3)	0·207 (3)	0·264 (3)
C(1)	35 (1)	229 (5)	245 (6)	0	6 (2)	0	0·168 (3)	0·182 (2)	0·200 (2)
C(2)	36 (1)	341 (6)	206 (7)	0	6 (2)	0	0·161 (3)	0·177 (3)	0·244 (2)
H(1)	54 (2)	367 (13)	366 (14)	0	0	83 (11)	0·203 (5)	0·212 (4)	0·266 (5)
H(2)	62 (2)	706 (17)	524 (14)	20 (5)	0 (4)	−332 (13)	0·194 (4)	0·228 (3)	0·392 (5)
H(3)	44 (2)	465 (16)	444 (17)	0	−8 (5)	0	0·191 (5)	0·242 (5)	0·285 (5)
DIDAB, neutron									
Br	32 (1)	144 (8)	428 (14)	0	0	0	0·159 (4)	0·163 (4)	0·237 (4)
N	30 (1)	160 (6)	176 (7)	0	0	0	0·152 (3)	0·159 (3)	0·167 (3)
O(1)	40 (1)	402 (11)	185 (10)	0	−4 (2)	0	0·155 (4)	0·183 (3)	0·265 (4)
O(2)	32 (1)	350 (11)	266 (10)	0	12 (3)	0	0·157 (3)	0·191 (4)	0·247 (4)
C(1)	31 (1)	186 (6)	195 (8)	0	7 (2)	0	0·153 (3)	0·168 (3)	0·180 (3)
C(2)	33 (1)	282 (8)	172 (8)	0	6 (2)	0	0·147 (4)	0·167 (3)	0·222 (3)
D(1)	45 (1)	274 (10)	318 (11)	0	0	113 (7)	0·165 (4)	0·194 (3)	0·249 (4)
H(2)	60 (2)	671 (23)	461 (18)	16 (6)	−1 (5)	−320 (17)	0·180 (5)	0·223 (4)	0·381 (6)
D(3)	38 (2)	375 (12)	393 (13)	0	−4 (3)	0	0·177 (4)	0·227 (4)	0·256 (4)
DIDAB, X-ray									
Br	38 (1)	193 (3)	463 (4)	0	0	0	0·177 (1)	0·183 (1)	0·246 (1)
N	34 (2)	197 (10)	183 (11)	0	0	0	0·155 (5)	0·169 (5)	0·185 (5)
O(1)	47 (2)	429 (13)	242 (9)	0	−5 (3)	0	0·177 (3)	0·198 (4)	0·274 (4)
O(2)	33 (2)	415 (10)	309 (10)	0	4 (3)	0	0·166 (4)	0·201 (3)	0·269 (3)
C(1)	38 (2)	202 (8)	249 (10)	0	10 (4)	0	0·170 (4)	0·188 (4)	0·189 (4)
C(2)	40 (2)	306 (12)	208 (9)	0	14 (4)	0	0·156 (4)	0·189 (5)	0·231 (5)

that reasonable standard deviations have been assigned to the coordinates. However, the non-zero intercepts of the plots might indicate small differences between the X-ray and neutron positions for both

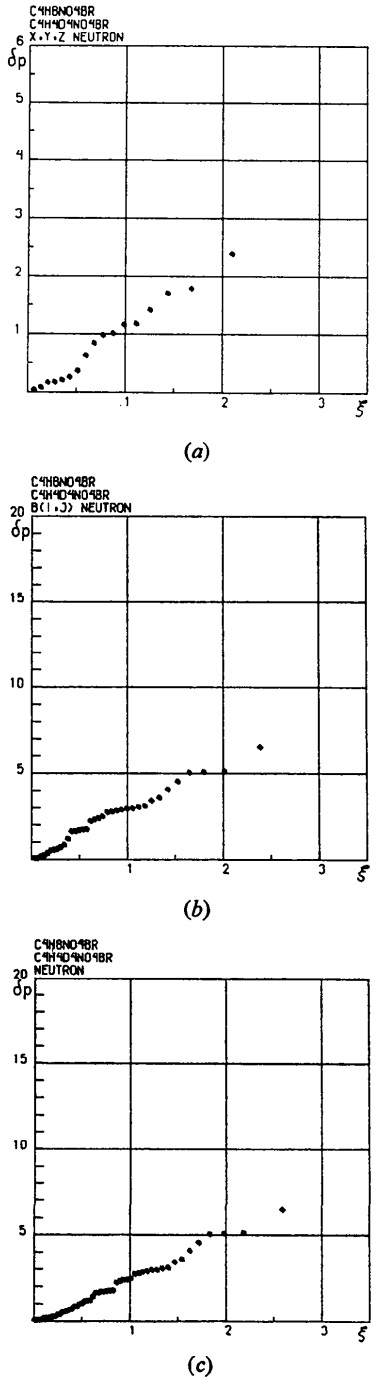

Fig. 1. Comparisons of the (*a*) positional, (*b*) thermal, (*c*) positional and thermal parameters in IDAB and DIDAB by half-normal probability plots. The residues compared and the type of radiation used are given above each plot. The slope and the intercept of the line defined by points with $\delta p < 5$ are: (*a*) 1·19, −0·11, (*b*) 2·91, 0·04, (*c*) 2·57, −0·21.

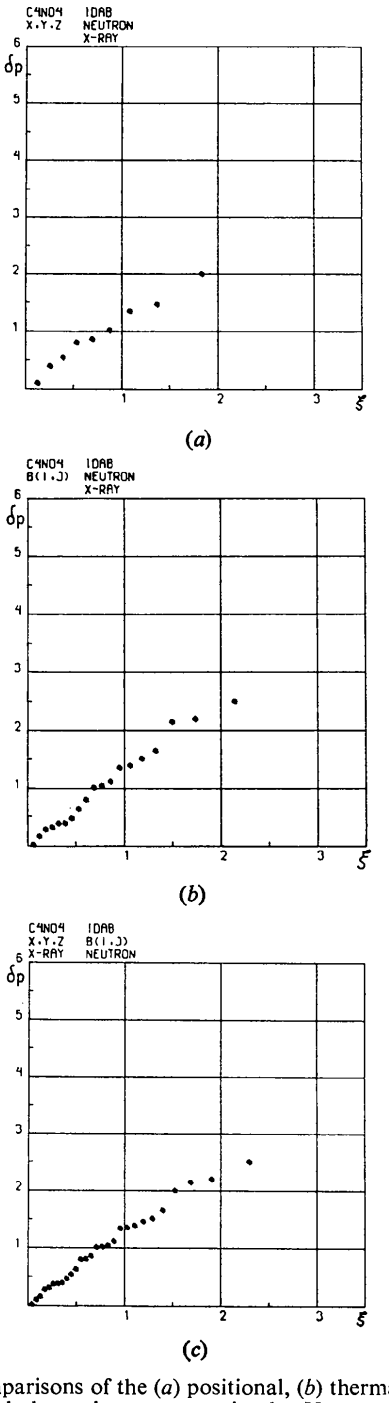

Fig. 2. Comparisons of the (*a*) positional, (*b*) thermal, (*c*) positional and thermal parameters in the X-ray and neutron studies of IDAB. The slope and the intercept of the line defined by points with $\delta p < 2$ are: (*a*) 1·04, 0·11, (*b*) 1·34, −0·04, (*c*) 1·24, 0·02.

IDAB and DIDAB. The plots for the thermal parameters show only small differences for IDAB. The differences are larger for DIDAB, which is shown by the larger slope and intercept as well as the non-linearity for points with $\delta p > 2$.

Description of the structure

The packing

IDAB and DIDAB are isostructural as shown by the half-normal probability plot [Fig. 1(*a*)]. The structure consists of Br^- ions and positively charged iminodiacetic acid ions, $[C_4H_8NO_4]^+$, with symmetry *mm*. The atoms of this ion are designated in Fig. 4. The non-hydrogen atoms of the iminodiacetic acid ion are located in the mirror planes at $y=\frac{1}{4}$ and $\frac{3}{4}$. These ions are connected by hydrogen bonds N–H···Br and O–H···Br forming zigzag-shaped layers stacked along c. The forces between the layers are van der Waals. The structure is shown in Fig. 5.

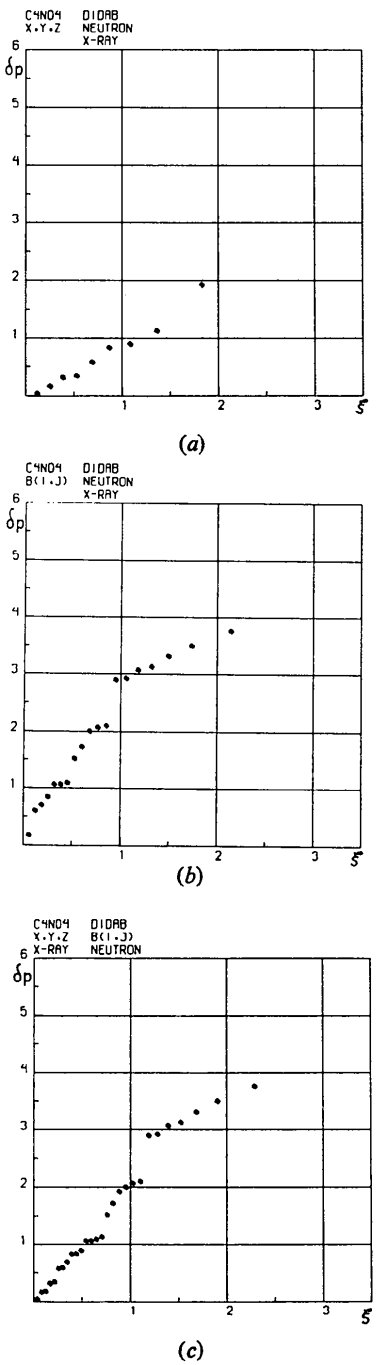

Fig. 3. Comparisons of the (*a*) positional, (*b*) thermal, (*c*) positional and thermal parameters in the X-ray and neutron studies of DIDAB. The slope and the intercept of the line defined by points with $\delta p < 2$ are: (*a*) 1·04, −0·14, (*b*) 2·57, 0·14, (*c*) 2·04, −0·06.

Selected interatomic distances and angles are given in Table 4. The shortest interlayer contacts are between $H(2^i)\cdots O(2^{ii})$ and $H(2^i)\cdots O(1)$. The H···O distances are 0·1 Å larger than the sum of their usually accepted van der Waals radii, which excludes hydrogen bonds of the type C–H···O.

The organic ion

The agreement in bond distances and angles for the non-hydrogen atoms within the organic ion is very satisfactory in the different structure determinations [Table 4(*b*)]. The dimensions agree well with a set of 'normal' structural parameters for this residue calculated from six different crystal structures determined by X-ray crystallography (Oskarsson, 1976). The C–H, N–H and O–H distances show an expected shortening in the X-ray studies caused by the pronounced asphericity of the electron distribution in these bonds.

The dynamics of the methylene hydrogen

The amplitude of the motion of the H atom in the methylene group relative to the C atom has been estimated by calculating the r.m.s. quantity $r_{C-H}(H)=[R^2_{C-H}(H)-R^2_{C-H}(C)]^{1/2}$, where R_{C-H} is the r.m.s. component of the total movement in the direction of the C–H bond. If a simple harmonic motion of the H atom is assumed the amplitude can be used to calculate the stretching frequency γ_{C-H}, by the relationship $\gamma_{C-H}=16{\cdot}8/r^2_{C-H}$ (Hamilton, 1969). The values of r_{C-H} [0·089 (7) and 0·108 (8) Å] correspond to the stretching frequencies 2100 and 1400 cm^{-1} for IDAB and DIDAB, respectively. Novak, Cotrait & Joussot-Dubien (1965) have studied the IR spectra of the Cl analogue of IDAB. A broad intense peak, centred at 2970 cm^{-1}, is ascribed to the C–H, N–H and O–H vibrations. This value is 2σ and 4σ away from the value obtained from the thermal parameters of the methylene group in IDAB and DIDAB, respectively. Therefore one may conclude that the thermal parameters of the methylene group are physically reasonable in IDAB but perhaps not in DIDAB and as a consequence this will be true also for the thermal parameters for the other atoms.

The hydrogen bonds

The H···Br distances are about 0·9 Å shorter than the sum of their van der Waals radii. This fulfils the geometrical criterion (Hamilton, 1968) that a hydrogen bond exists if the H···B distance is 0·2 Å or more shorter than the sum of the van der Waals radii.

Some geometrical characteristics of the hydrogen bonds are shown in Table 4(*c*). The O···Br and N···Br distances are 0·07 and 0·08 Å shorter than the average values for these hydrogen bond distances calculated from crystal structures reported through 1969 (Pimentel & McClellan, 1971). The short H(D)···Br, O···Br and N···Br distances indicate fairly strong hydrogen bonds, which is further supported by the moderate deviations from linearity of these bonds.

From a valence bond model one would expect the proton to approach the Br^- ion in the direction of one of the lone pairs. Simple hybridization concepts and Gillespie & Nyholm electron-pair repulsion theory then predict H···Br···H angles close to 109°. No such preferred tetrahedral arrangement of the H(D) atoms around the Br^- ion is found, which indicates that the hydrogen bonds should be essentially electrostatic in nature.

There are no significant differences in the geometry of the hydrogen bonds in IDAB and DIDAB, since the largest discrepancies are about 1σ. The unit cell dimensions in DIDAB are 0·0103 (39), 0·0035 (17) and 0·0063 (14) Å smaller for *a*, *b* and *c*, respectively, compared to IDAB. The differences range from 2σ to $4{\cdot}5\sigma$. These discrepancies are also too small to show clearly that there are real differences in the hydrogen-bond systems of IDAB and DIDAB. The effect observed in the Cl analogue was three to four times larger (Oskarsson, 1974*c*).

(X–N) difference Fourier syntheses

The positions and thermal motions of the nuclei derived from neutron diffraction data can be used in combination with the X-ray structure factors to ob-

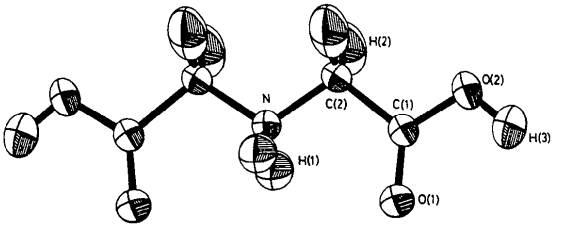

Fig. 4. Designation of the atoms in the positively charged iminodiacetic acid ion.

Table 4. *Selected interatomic distances* (Å) *and angles* (°) *with e.s.d.'s in IDAB and DIDAB*

The superscripts (i)–(vi) indicate the following equivalent sites in the structure: (i) x,y,z; (ii) $1-x,1-y,1-z$; (iii) $\frac{1}{2}-x,y,z$; (iv) $x,\frac{1}{2}-y,z$; (v) $x,1+y,z$; (vi) $x-\frac{1}{2},1-y,1-z$. The data for IDAB (X-ray) are taken from Oskarsson (1973).

	IDAB, X-ray	IDAB, neutron	DIDAB, X-ray	DIDAB, neutron
(*a*) Interlayer distances				
$H(2^i)\cdots O(2^{ii})$	2·741 (51)	2·700 (6)	2·799 (39)	2·695 (6)
$H(2^i)\cdots O(1)$	2·787 (39)	2·697 (6)	2·768 (28)	2·706 (5)
$O(1)\cdots O(2^i)$	3·457 (5)	3·460 (4)	3·452 (4)	3·452 (4)
(*b*) The iminodiacetic acid ion				
N—C(2)	1·480 (5)	1·476 (2)	1·474 (4)	1·476 (2)
C(1)–C(2)	1·505 (6)	1·509 (2)	1·503 (5)	1·508 (3)
C(1)–O(1)	1·199 (5)	1·201 (2)	1·197 (4)	1·198 (3)
C(1)–O(2)	1·320 (5)	1·313 (3)	1·321 (4)	1·312 (3)
N—H(1)	0·98 (6)	1·026 (4)	0·90 (4)	1·034 (3)
C(2)–H(2)	0·94 (5)	1·078 (4)	0·92 (4)	1·071 (5)
O(2)–H(3)	0·73 (4)	0·978 (4)	0·65 (4)	0·983 (4)
$C(2)–N—C(2^{iii})$	114·2 (4)	113·8 (2)	114·0 (3)	113·6 (2)
N—C(2)–C(1)	108·8 (3)	109·0 (1)	108·7 (3)	108·7 (2)
C(2)–C(1)–O(2)	111·2 (3)	111·8 (2)	111·1 (3)	111·5 (2)
C(2)–C(1)–O(1)	123·1 (4)	122·8 (2)	123·6 (3)	123·0 (2)
O(2)–C(1)–O(1)	125·7 (4)	125·4 (2)	125·3 (3)	125·5 (2)
C(2)–N—H(1)	110 (2)	109·1 (1)	111 (1)	109·2 (1)
$H(1)–N—H(1^{iv})$	104 (7)	106·6 (4)	199 (5)	106·1 (3)
N—C(2)–H(2)	111 (3)	109·6 (2)	109 (2)	109·5 (3)
C(1)–C(2)–H(2)	104 (3)	110·6 (2)	109 (2)	110·3 (3)
$H(2)–C(2)–H(2^{iv})$	104 (3)	107·6 (4)	112 (4)	108·4 (5)
C(1)–O(2)–H(3)	118 (5)	110·0 (3)	112 (4)	109·5 (3)
(*c*) The hydrogen bonds				
N·····Br	3·289 (2)	3·288 (1)	3·291 (2)	3·288 (2)
$H(1^{iv})\cdots Br$	2·20 (4)	2·285 (4)	2·43 (4)	2·277 (3)
$N———H(1^{iv})\cdots Br$	164 (5)	165·6 (3)	162 (3)	165·3 (2)
$O(2^{ii})\cdots Br$	3·216 (3)	3·211 (2)	3·216 (3)	3·214 (3)
$H(3^{ii})\cdots Br$	2·49 (7)	2·264 (4)	2·59 (4)	2·265 (3)
$O(2^{ii})—H(3^{ii})\cdots Br$	174 (7)	162·6 (4)	167 (5)	162·2 (3)
$H(1^{iv})\cdots Br\cdots\cdots H(1^v)$	136 (3)	135·3 (2)	136 (2)	135·4 (2)
$H(3^{ii})\cdots Br\cdots\cdots H(3^{vi})$	127 (3)	135·4 (2)	130 (2)	135·6 (2)
$H(1^{iv})\cdots Br\cdots\cdots H(3^{ii})$	100 (1)	98·30 (5)	99·2 (5)	98·24 (3)

tain information about deviations from spherical symmetry of the electron distribution around the atoms (Coppens, 1974). The quantities $F_{o,X}-F_{c,N}$ are used as coefficients in Fourier summations. $F_{o,X}$ is the observed X-ray structure factor amplitude with the calculated sign, $F_{c,N}$ is the structure factor calculated from spherical free-atom X-ray form factors and the atomic parameters from the neutron diffraction analysis. Before calculating the difference maps the $F_{o,X}$ were corrected for extinction, with the isotropic extinction parameter obtained from the X-ray refinement and adjusted to a 'correct' scale by a few cycles of least-squares refinement on the scale factor alone. When anomalous scatterers are present the scattering factor is a complex function, $f=f_0+f'+f''$. Therefore the structure factors are also complex for centrosymmetric structures and this will introduce errors in the electron density maps (Del Pra & Mammi, 1972): $F=\sum(f_0+f')Q\cos 2\pi\mathbf{hr}+i\sum f''Q\cos 2\pi\mathbf{hr}$; $F=F_r+iF_i$ and $|F|=(F_r^2+F_i^2)^{1/2}$, where Q is a temperature factor. The observed structure factors are thus not the correct coefficients for the electron density function. However, the correct coefficients can be approximated by $F'_{o,X}=F'_c|F_{o,X}|/|F_c|$, where F'_c is a structure factor calculated with f_0 in place of f (Templeton, 1955). Two sets of difference maps were calculated for IDAB, one with $F_{o,X}$ and one with $F'_{o,X}$ (Fig. 6). The general features of the two sets of electron density maps are very similar. The main difference is a smaller electron density in the maps calculated with $F'_{o,X}$. This decrease is about 5% in most of the bonds within the organic ion and 20% in the vicinity of the Br^- ion. It is concluded that the correction for anomalous dispersion slightly improves the quality of the difference maps.

The maximum error in the maps is estimated as 0·25 e $Å^{-3}$ from the noise level in regions where the electron density is expected to be zero. For centrosymmetric structures the average standard deviations in the maps can be approximated by

$$\langle\sigma^2(\varrho_{X-N})\rangle=\frac{2}{V^2}\left[\sum\sigma^2(F_{o,X})+\left(\frac{\langle f_i\rangle}{\langle b_i\rangle}\right)^2\sigma^2(F_{o,N})\right],$$

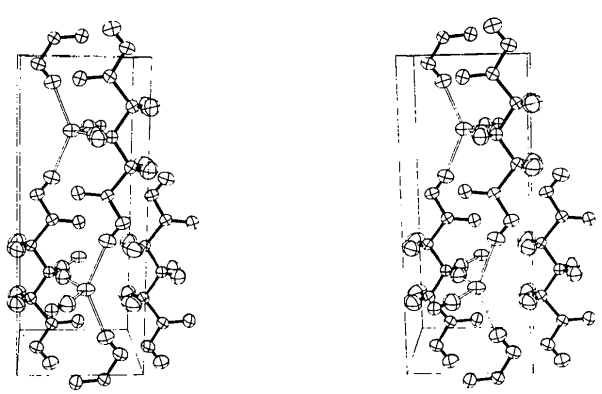

Fig. 5. A stereoscopic pair of drawings showing the structure of IDAB. The *b* axis points towards the reader, *c* to the right, and *a* upwards.

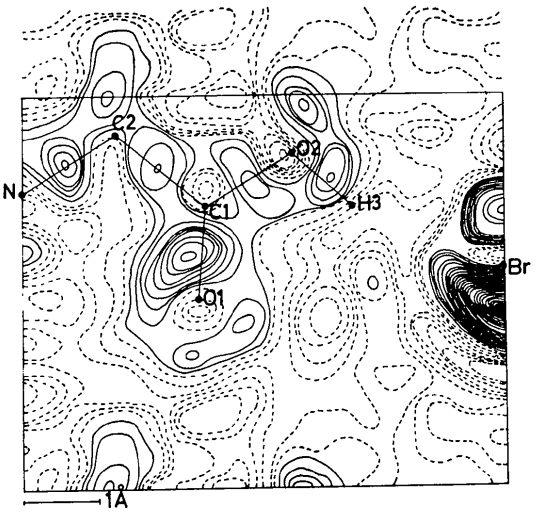

(*a*)

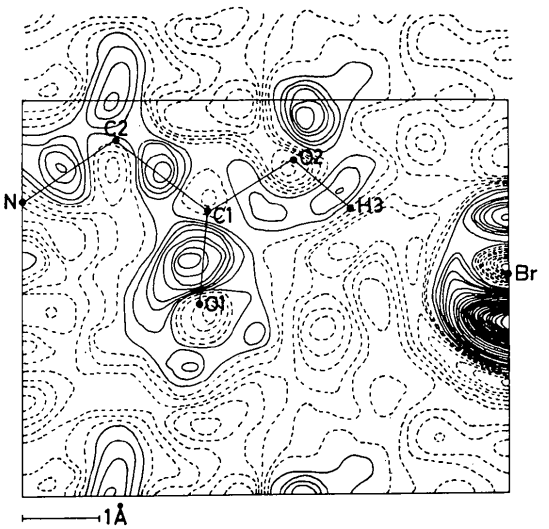

(*b*)

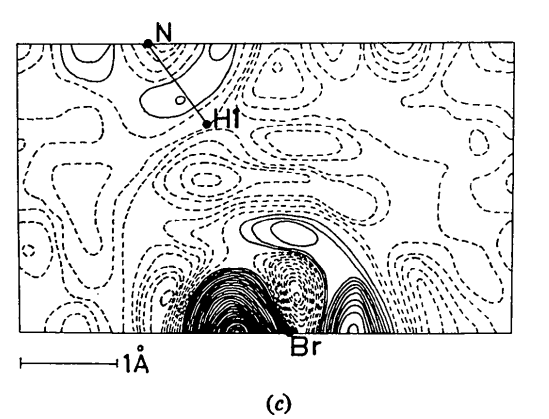

(*c*)

Fig. 6. (X–N) difference electron density maps. The contours are drawn at 0·05 e $Å^{-3}$ intervals, zero and negative levels are represented by dashed lines. (*a*) The plane at $y=\frac{1}{4}$, uncorrected data. (*b*) The plane at $y=\frac{1}{4}$. The $|F_o|$ used have been corrected for anomalous dispersion. (*c*) The plane at $x=\frac{1}{4}$, corrected data.

where f_i is the X-ray form factor multiplied by the amplitude of the radiation scattered by one electron and b_i is the scattering length for thermal neutrons (Coppens, 1974). For first row elements $\langle f_i \rangle \simeq \langle b_i \rangle$ but for compounds containing heavier elements these two factors will increase the average standard deviation.

Another factor of importance in the discussion of the comparatively large error observed in the maps is that errors accumulate in special positions (Cruickshank & Rollett, 1953).

The electron density maps reported in Fig. 6 cannot be used for a quantitative discussion because of the large error involved. For the same reason no maps are reported for DIDAB.

Intuitively reasonable electron densities are found close to the centres of the covalent bonds. The electronic structures of the two O atoms in a carboxylic group can be described as $(1s)^2(2sp^2)^1(2sp^2)^2(2sp^2)^2(2p\pi)^1$ (the carbonyl O atom) and $(1s)^2(2sp^2)^1(2sp^2)^1(2sp^2)^2(2p\pi)^2$ (the carboxyl O atom), which imply two and one lone pairs, respectively, in the plane of the organic ion. This is in agreement with the observed electron density around the O atoms. The peak maximum in the O–H bond is at the same position as obtained for H(3) in the X-ray structure refinement. The deviation from spherical electron density distribution is thus compensated by a shift of H towards the O atom in the least-squares procedure. It is interesting to note that in the compounds $C_4H_8NO_4X$ this shift increases in the series $F < Cl < Br < I$ (Oskarsson, 1973, 1974*a*,*b*). No such effect is observed in the N–H bond. Both the OH···Br and NH···Br bonds should be essentially electrostatic in nature since the distances with negligible electron density extend over *ca* 1 Å in these bonds.

I am indebted to Drs J. Albertsson and R. Tellgren for valuable help and enlightening discussions. This work has been supported by the Swedish Natural Science Research Council.

References

ABRAHAMS, S. C. & KEVE, E. T. (1971). *Acta Cryst.* A**27**, 157–165.

ALBERTSSON, J. (1974). Private communication.

BACON, G. E. (1972). *Acta Cryst.* A**28**, 357–358.

BELL, R. P. (1974). *Chem. Soc. Rev.* **3**, 513–544.

COPPENS, P. (1974). *Acta Cryst.* B**30**, 255–261.

COPPENS, P. & HAMILTON, W. C. (1970). *Acta Cryst.* A**26**, 71–83.

CRUICKSHANK, D. W. J. & ROLLETT, J. S. (1953). *Acta Cryst.* **6**, 705–707.

DEL PRA, A. & MAMMI, M. (1972). *Acta Cryst.* A**28**, 65–69.

HAMILTON, W. C. (1968). *Structural Chemistry and Molecular Biology*, edited by A. RICH & N. DAVIDSON, p. 466. San Francisco & London: Freeman.

HAMILTON, W. C. (1969). *Molecular Dynamics and Structure of Solids*, edited by R. S. CARTER & J. J. RUSH. National Bureau of Standards Special Publication 301, p. 195.

HAMILTON, W. C. & ABRAHAMS, S. C. (1972). *Acta Cryst.* A**28**, 215–218.

HANSON, H. P., HERMAN, F., LEA, J. D. & SKILLMAN, S. (1964). *Acta Cryst.* **17**, 1040–1044.

International Tables for X-ray Crystallography (1974). Vol. IV, p. 149. Birmingham: Kynoch Press.

NOVAK, A., COTRAIT, M. & JOUSSOT-DUBIEN, J. (1965). *Bull. Soc. Chim. Fr.* pp. 1808–1812.

OSKARSSON, Å. (1973). *Acta Cryst.* B**29**, 1747–1751.

OSKARSSON, Å. (1974*a*). *Acta Cryst.* B**30**, 780–783.

OSKARSSON, Å. (1974*b*). *Acta Cryst.* B**30**, 1184–1188.

OSKARSSON, Å. (1974*c*). *Acta Chem. Scand.* A**28**, 250–252.

OSKARSSON, Å. (1976). *Acta Chem. Scand.* B**30**, 125–132.

PIMENTEL, G. C. & MCCLELLAN, A. L. (1971). *Ann. Rev. Phys. Chem.* **22**, 347–385.

REES, B. & COPPENS, P. (1973). *Acta Cryst.* B**29**, 2516–2528.

STEWART, R. F., DAVIDSON, E. R. & SIMPSON, W. T. (1965). *J. Chem. Phys.* **42**, 3175–3187.

TEMPLETON, D. H. (1955). *Acta Cryst.* **8**, 842.

ZACHARIASEN, W. H. (1967). *Acta Cryst.* **23**, 558–564.